Behavioral and neural correlates to multisensory detection of sick humans

Christina Regenbogen[a,b,c,1], John Axelsson[a,d], Julie Lasselin[a,d,e], Danja K. Porada[a], Tina Sundelin[a,f], Moa G. Peter[a], Mats Lekander[a,d], Johan N. Lundström[a,g,h,2], and Mats J. Olsson[a,1,2]

[a]Division of Psychology, Department of Clinical Neuroscience, Karolinska Institutet, 171 77 Stockholm, Sweden; [b]Department of Psychiatry, Psychotherapy and Psychosomatics, Medical School, Rheinisch-Westfälische Technische Hochschule Aachen, 52074 Aachen, Germany; [c]Jülich Aachen Research Alliance - BRAIN Institute 1: Structure Function Relationship, Jülich Aachen Research Alliance, 52425 Juelich, Germany; [d]Stress Research Institute, Stockholm University, 106 91 Stockholm, Sweden; [e]Institute of Medical Psychology and Behavioral Immunobiology, Universitätsklinikum Essen, 45147 Essen, Germany; [f]Department of Psychology, Stockholm University, 106 91 Stockholm, Sweden; [g]Monell Chemical Senses Center, Philadelphia, PA 19104; and [h]Department of Psychology, University of Pennsylvania, Philadelphia, PA 19104

Edited by Noam Sobel, Weizmann Institute, Rehovot, Israel, and accepted by Editorial Board Member Randolph Blake April 26, 2017 (received for review October 26, 2016)

Throughout human evolution, infectious diseases have been a primary cause of death. Detection of subtle cues indicating sickness and avoidance of sick conspecifics would therefore be an adaptive way of coping with an environment fraught with pathogens. This study determines how humans perceive and integrate early cues of sickness in conspecifics sampled just hours after the induction of immune system activation, and the underlying neural mechanisms for this detection. In a double-blind placebo-controlled crossover design, the immune system in 22 sample donors was transiently activated with an endotoxin injection [lipopolysaccharide (LPS)]. Facial photographs and body odor samples were taken from the same donors when "sick" (LPS-injected) and when "healthy" (saline-injected) and subsequently were presented to a separate group of participants ($n = 30$) who rated their liking of the presented person during fMRI scanning. Faces were less socially desirable when sick, and sick body odors tended to lower liking of the faces. Sickness status presented by odor and facial photograph resulted in increased neural activation of odor- and face-perception networks, respectively. A superadditive effect of olfactory–visual integration of sickness cues was found in the intraparietal sulcus, which was functionally connected to core areas of multisensory integration in the superior temporal sulcus and orbitofrontal cortex. Taken together, the results outline a disease-avoidance model in which neural mechanisms involved in the detection of disease cues and multisensory integration are vital parts.

body odor | lipopolysaccharide | endotoxin | sickness cues | disease avoidance

Social interactions serve adaptive purposes (1), but these interactions can be dangerous and potentially fatal if the conspecifics host an infectious disease. The significance of the pathogenic threat is evidenced by the fact that genes relating to immunity are evolutionary hotspots where the defense against pathogens is a leading cause of genetic adaptation (2). It has recently been proposed that animals and humans have developed adaptations complementing the physiological immune system through reducing both exposure to and the toll of infection (3, 4). A central set of adaptations refers to disease avoidance, that is, an ability to detect and avoid possible pathogenic threats in the environment. Here, the exposure to disease cues in other individuals is proposed to facilitate certain cognitive and emotional responses, consequently provoking social avoidance and certain immune markers (3, 5). Many animals can detect sick individuals via odor cues such as volatiles in urine and feces (6), and sickness detection leads to constrained social investigations in healthy conspecifics, possibly minimizing disease transmission. However, only a few studies have assessed a sensory-mediated sickness-detection mechanism in humans, and essentially nothing is known about the neural mechanisms underlying the detection of sick individuals and potential subsequent social avoidance tendencies toward them.

Still, several findings suggest that visual cues such as skin coloration (i.e., redness) are indeed important when judging apparent health of others from facial photographs (7), that disease-related visual stimuli (such as seeing photos of a person sneezing) elicit an aggressive immune response (8), and that exposure to disgust-inducing visual stimuli increases immune markers in the oral cavity (5). Similarly, different patient groups are associated with characteristic body odors (9, 10). However, none of these studies has manipulated acute health status, and therefore they have not been able to establish any evidence for causality between sickness and detectable cues, nor have they investigated these cues soon after the induction of a systemic sickness response.

A possible way to study sickness detection in and by humans is the experimental induction of an inflammatory response in otherwise healthy subjects, using endoxin [lipopolysaccharide (LPS)] injections, which activates a robust sickness response (11). Recent data indicate that the sickness response makes individuals' body odor more aversive (12) and also influences their walking gate pattern, leading naive participants to rate these individuals as less healthy (13).

Although LPS induces a reliable sickness response, the effects on overt behavior can be subtle (13). In addition, odor cues are often difficult to assess consciously (14–16). With this background, we would expect visual and olfactory cues of LPS-induced sickness

Significance

In the perpetual race between evolving organisms and pathogens, the human immune system has evolved to reduce the harm of infections. As part of such a system, avoidance of contagious individuals would increase biological fitness. The present study shows that we can detect both facial and olfactory cues of sickness in others just hours after experimental activation of their immune system. The study further demonstrates that multisensory integration of these olfactory and visual sickness cues is a crucial mechanism for how we detect and socially evaluate sick individuals. Thus, by motivating the avoidance of sick conspecifics, olfactory–visual cues, both in isolation and integrated, may be important parts of circuits handling imminent threats of contagion.

Author contributions: C.R., J.A., J.L., D.K.P., T.S., M.G.P., M.L., J.N.L., and M.J.O. designed research; C.R., D.K.P., M.G.P., J.N.L., and M.J.O. performed research; J.N.L. contributed new reagents/analytic tools; C.R. analyzed data; and C.R., J.A., J.L., T.S., M.L., J.N.L., and M.J.O. wrote the paper.

The authors declare no conflict of interest.

This article is a PNAS Direct Submission. N.S. is a guest editor invited by the Editorial Board.

See Commentary on page 6157.

[1]To whom correspondence may be addressed. Email: cregenbogen@ukaachen.de or mats.j.olsson@ki.se.

[2]J.N.L. and M.J.O. contributed equally to this work.

This article contains supporting information online at www.pnas.org/lookup/suppl/doi:10.1073/pnas.1617357114/-/DCSupplemental.

to be rather vague. It is clear, however, that the integration of weak specific signals from individual sensory systems improves the accuracy and speed of detection (17–19). To assess multisensory facilitation of sickness-cue detection and its neural correlates, we investigated changes in whole-brain activation in response to the presentation of sick and healthy faces combined with the presentation of body odors of sick and healthy individuals, and we assessed "liking behavior" toward the faces. Liking represents a central facilitator of human behavior, with clear implications for when to approach and affiliate with others (20, 21). Accordingly, reduced liking in response to the perception of subtle cues of sickness may indicate a behavioral tendency for the initiation of an overt behavioral defense against disease in humans.

Facial photographs and body odors were sampled from 18 individuals (nine women), here referred to as "donors," who had participated in a double-blind placebo-controlled crossover design study. Samples were taken when donors were "sick" (after LPS injection at a dose of 2.0 ng/kg body weight) and when they were "healthy" (after saline injection) (22). A second group of naive participants ($n = 30$) was exposed to the photos and body odors while their cerebral responses were recorded using fMRI. Visual stimuli, i.e., photographs of healthy or sick donors' faces displayed on a computer screen, were presented in combination with body odor from either sick or healthy donors, or a control odor (an unused sampling pad; all odors were presented to the nose by an olfactometer). Participants were instructed to focus on the face and rate spontaneously how much they liked the depicted person.

We hypothesized that sick faces and faces paired with sick body odors would render less liking of the person compared with their respective healthy counterparts and that congruent sickness cues from multiple sensory channels (i.e., sick faces paired with sick body odor) would elicit the lowest liking ratings. We further predicted that sickness cues compared with healthy ones would evoke enhanced blood oxygen level-dependent (BOLD) changes in the odor-perception network (piriform cortex, orbitofrontal cortex, and amygdala) and in the face-perception network (fusiform gyrus, inferior and superior frontal gyrus, and amygdala). This prediction was based on previous studies demonstrating sickness-driven changes in body odors (12) and facial appearance (23) and on several studies indicating salience- and threat-driven changes in the respective olfaction- (24) and vision- (25) processing networks.

We also investigated the combined multisensory olfactory–visual sickness signal in areas that detect own sickness and, potentially, sickness in others, such as the orbitofrontal cortex, posterior cingulate cortex, and insula (26). We specifically tested whether the neural correlates of combined olfactory–visual sickness cues would cause activation to and above the sum (superadditive) of the olfactory and visual sickness cue profiles, thus representing the presence of multisensory integration of human sickness signals.

Results

Behavior.

Effects of sickness cues in face and odor on liking. The results of a repeated-measures ANOVA determining sickness-dependent effects on liking ratings of the presented faces (Fig. 1) showed a main effect of face [$F(1,29) = 24.85$, $P < 0.001$, $\eta_p^2 = 0.46$], a main effect of odor [$F(2,58) = 3.56$, $P = 0.035$, $\eta_p^2 = 0.11$], and no significant interaction [$F(2, 58) = 0.42$, $P = 0.66$, $\eta_p^2 = 0.01$]. The main effect of face (Fig. 1*A*) indicated lower liking of sick than of healthy faces, regardless of the odor type (sick, healthy, or control) presented with the face. Pairwise tests of odor (Fig. 1*B*) indicated that faces, regardless of the type (sick, healthy), paired with sick body odor were less liked than faces paired with the control odor [$t(29) = 2.11$, $P = 0.04$, $d = 0.23$] and a statistical trend for their being less liked than faces paired with healthy body odor [$t(29) = 1.68$, $P = 0.10$, $d = 0.12$]. The comparison of faces paired with healthy body odor vs. faces paired with control odor was not significant [$t(29) = -1.49$, $P = 0.18$, $d = 0.11$].

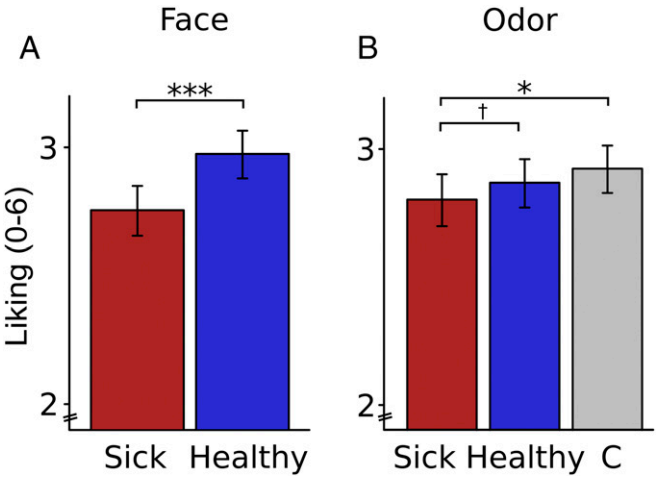

Fig. 1. Bar graphs depict participants' liking ratings (mean ± SEM) of the presented person as a function of the health status of faces (*A*) and of odors (*B*). Shorter bars indicate lower liking. ***$P < 0.001$, *$P = 0.04$, $^{\dagger}P = 0.10$. C, control odor.

Postscanning ratings of separately presented faces and odors. After scanning, faces and odors were rated along further subjective dimensions, this time following separate unimodal presentations. The results of a repeated-measures ANOVA determining sickness-dependent effects on perceptual ratings of the presented odors (Fig. 2, *Upper Row*) showed a significant main effect of odor for pleasantness [$F(2,58) = 8.31$, $P = 0.001$, $\eta_p^2 = 0.22$]. Pairwise tests indicated that participants rated both sick [$t(29) = 3.98$, $P < 0.001$, $d = 0.87$] and healthy [$t(29) = 3.022$, $P = 0.005$, $d = 0.67$] body odor as less pleasant than the control odor. The comparison between sick and healthy body odor was not statistically significant [$t(29) = 0.66$, $P = 0.52$, $d = 0.14$]. For health ratings, there was a significant main effect of odor [$F(2,58) = 4.78$, $P = 0.01$, $\eta_p^2 = 0.14$]. Both sick [$t(29) = 2.75$, $P = 0.01$, $d = 0.69$] and healthy [$t(29) = 2.42$, $P = 0.02$, $d = 0.61$] body odor received lower health ratings than the control odor but did not differ significantly from each other [$t(29) = 0.06$, $P = 0.95$, $d = 0.02$]. For intensity ratings of odors, there was no significant effect in intensity between the three odor conditions [$F(2,58) = 2.61$, $P = 0.08$, $\eta_p^2 = 0.08$].

Paired t tests on judgments of sick and healthy faces (Fig. 2, *Lower Row*) carried out after scanning showed significant differences between healthy and sick faces regarding attractiveness, health, and desired social interaction ratings. Photographs obtained during acute sickness were on average rated as less attractive [$t(29) = 4.59$, $P < 0.001$, $d = 0.48$)], less healthy [$t(29) = 7.18$, $P < 0.001$, $d = 1.29$], and less socially desirable [$t(29) = 4.64$, $P < 0.001$, $d = 0.37$] than photographs taken during the placebo (saline) treatment.

Functional Imaging.

Effects of sickness in face and odor on whole-brain activation. In a whole-brain analysis, we determined the neural signatures of visual and olfactory sickness cues, respectively (Fig. 3). We first determined the neural network relating to the perception of sick in comparison with healthy faces (i.e., visual sickness) by contrasting all presentations of sick faces against all presentations of healthy faces (across all body odor pairings). The contrast visual sickness was related to a significant activation in the right superior frontal gyrus (dorsal part) and the left middle frontal gyrus (ventral part, bordering on the frontal pole), as well as the right posterior insula and the right middle cingulate cortex (Fig. 3*A* and Table S1). Please refer to Fig. S1 for time course plots of the BOLD response during all contrasts. We then determined the neural network relating to the perception of sick vs. healthy

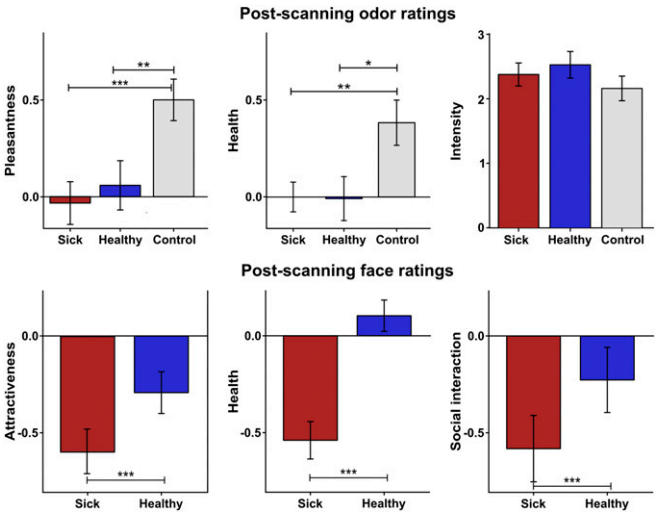

Fig. 2. Bar graphs depict postscanning ratings of all faces and odors (mean ± SEM). ***$P < 0.001$, **$P < 0.01$, *$P < 0.05$.

body odor (i.e., olfactory sickness) by contrasting all presentations with a sick body odor against all presentations with a healthy body odor (across all face pairings). The olfactory sickness contrast was related to significant activation in the bilateral mediodorsal thalamus, the right posterior orbital and orbitofrontal cortex, the right entorhinal/piriform cortex, the bilateral inferior frontopolar gyrus, and in the left middle frontal gyrus (ventral part) (Fig. 3*B* and Table S1).

Effects of multisensory sickness on whole-brain activation. We then assessed whether the brain demonstrated integrative neural processing of the olfactory and visual sickness cues (Fig. 4). We first focused on additive (in contrast to superadditive) integration by determining the neural signature for olfactory–visual sickness cues by directly comparing the olfactory–visual sickness condition with the olfactory–visual health condition. The contrast olfactory–visual sickness was related to three activation clusters in the right and left superior frontal gyrus (all in the dorsal part) and to activation in the left middle frontal gyrus (ventral part), the left inferior frontal gyrus (stretching into the temporal pole), the right orbitofrontal cortex, the bilateral mediodorsal thalamus, and the left cerebellum (Fig. 4*A* and Table S1).

To assess whether and where multisensory sickness cues would meet the criterion of superadditivity, we contrasted the multisensory sickness condition to the sum of the unimodal sickness cues. This superadditive sickness contrast, testing for activation that would exceed the sum of activations associated with olfactory and visual sickness, was present in bilateral lingual (visual cortex) and bilateral middle occipital gyri, in the right parietal sulcus and gyrus, and in the left motor cortex and the left cerebellum (Fig. 4*B* and Table S1).

A psychophysiological interaction (PPI) analysis was conducted to test functional connectivity of the intraparietal sulcus (IPS), a central area for multisensory integration, during superadditive sickness (Fig. 5). The aim was to identify brain regions in which activity is more related to activity in the IPS in the context of multisensory integration of sickness cues than in the context of a mere summation of visual and olfactory sickness cues.

During superadditive sickness, we found increased functional connectivity between the IPS and a network consisting of bilateral inferior and superior temporal cortices (anterior and posterior part), right inferior parietal lobe, bilateral anterior and middle cingulate cortices, bilateral precuneus, primary visual cortex, and right fusiform cortex (Fig. 5 and Table S1).

Discussion

This work provides information on the neural mechanisms underlying the detection of sick individuals. We can demonstrate that individuals' liking behavior toward another person changes as a function of the underlying inflammatory activation in response to a bacterial-type stimulus in these persons and, further, that individuals on average rate sick persons as less healthy, attractive, and socially desirable based on visual cues. The reduced willingness of humans to socialize with sick individuals at the behavioral level supports the notion of a behavioral defense response that could lower the probability for contagion. Importantly, these behavioral effects are already evident 2 h after the onset of an immune response. Although these results suggest that we can distinguish sick from healthy states at an early stage, side-by-side discrimination between sick and healthy individuals should be performed to gauge the sensitivity and specificity of disease detection in this context. Moreover, we can demonstrate that visual and olfactory sickness cues yield increased activation in their respective olfactory sensory and visual face processing cortices. Finally, we present evidence for multisensory integration of sickness cues in the intraparietal sulcus, a core multisensory integration area, thus indicating that the brain can extract and process amodal sickness cues.

Our first aim was to deconstruct olfactory–visual sickness into its unisensory contributions. Olfactory sickness (Fig. 3*B*) was related to increased activation of the mediodorsal thalamus (MDT) and of the odor perception network (27), including the orbitofrontal cortex (OFC), the entorhinal/piriform cortex, and the inferior frontopolar and middle frontal gyrus. The odor perception network is susceptible to attention and learning (28), as well as threat processing (24). Pertinent to this study, it has been shown that the olfactory cortex (piriform cortex, OFC, amygdala) stores threat codes as acquired associative representations formed via aversive life experiences.

The role of the MDT is less clear. Although olfactory processing has a nonobligatory thalamic relay (e.g., in contrast to vision), thalamic lesions cause impairments in odor functioning (29), i.e., in identification and in evaluation of pleasantness. Moreover, it has been suggested that thalamic nuclei receive indirect olfactory input from olfactory cortex (30). That odor pleasantness is associated with thalamic activity (31) is of further interest, given that in our data the pleasantness of the sick body odor was reduced compared with the control pad but was only insignificantly reduced compared with the healthy body odor. This result did not replicate previous findings showing that sick body odors are perceived as stronger and more unpleasant than healthy ones (12). A

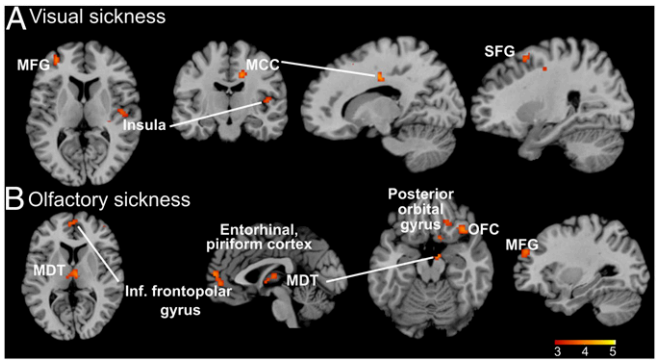

Fig. 3. Whole-brain activation to visual sickness (*A*) and olfactory sickness (*B*) shown as t-contrasts from a random-effects GLM. All activation maps are depicted in neurological convention. The color bar depicts t-values of local maxima peak activation. MCC, middle cingulate cortex; MDT, mediodorsal thalamus; MFG, middle frontal gyrus; OFC, orbitofrontal cortex; SFG, superior frontal gyrus.

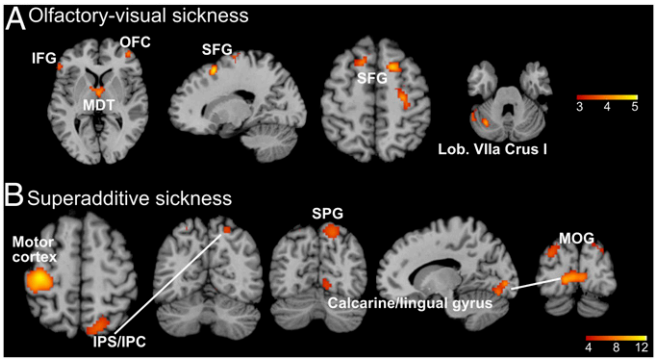

Fig. 4. Whole-brain activation to olfactory–visual sickness (*A*) and superadditive sickness (*B*); t-contrasts are from a random-effects GLM. IFG, inferior frontal gyrus; IPC, inferior parietal gyrus; IPS, inferior parietal sulcus; MDT, mediodorsal thalamus; MOG, middle occipital gyrus; OFC, orbitofrontal cortex; SFG, superior frontal gyrus; SPG, superior parietal gyrus.

possible explanation for our results may be that body odors presented by an olfactometer, as ours were, are typically perceived as weaker than odors presented from head-space saturated jars [as done in a previous study by our group (12)]; this notion is supported by the sick and healthy body odors in our not rated being rated as more intense than the control pads in this study.

Even though body odors were weak, and no clear perceptual differences between healthy and sick body odor were observed, it is interesting that activations by olfactory sickness cues were found. This pattern supports previous findings showing that the effects of exposure to body odors do not depend on clearly conscious stimulation (14, 15). Consequently, the complete odor network may relay threat-related cues to higher cortical areas and thereby may serve disease avoidance at later, potentially more conscious stages, eventually causing behavioral adaptation. We also note that an olfactory threat signal need not be perceptually distinct to be processed by the brain (15, 16). Future studies should assess the neural changes associated with clearly conscious perception of odor sickness cues.

As noted, the photographs of sick faces were indeed related to significantly reduced liking, health, attractiveness, and willingness for social interaction as compared with the photographs of healthy faces, thus supporting the avoidance of sick individuals on a behavioral level. The study therefore provides evidence that humans have the ability to detect early signs of sickness by merely observing facial photos of acutely sick individuals. On a neural level, visual sickness (Fig. 3*A*) activated the superior and middle frontal gyrus, the posterior insula, and the middle cingulate cortex. The superior and middle frontal gyrus seemed to reflect sickness-driven visual processing in parts of the cortical face-processing network (32). They may, together with the insula, amygdala, and the middle cingulate cortex, point toward the presence of facial emotion recognition (32) or to shared neural representations (33) of a firsthand experience of an emotion-like state such as feeling sick (26). Although this interpretation remains speculative because participants lacked an actual firsthand experience, the donors depicted in the facial photographs felt more sick and anxious after LPS treatment than after placebo saline treatment, as reported earlier (22). Therefore the interpretation that the activations involved in observing infected humans in discomfort and potentially in pain are, to some degree, related to the activations involved in actually being sick and potentially experiencing pain oneself may not be too far-fetched and should be investigated further in future investigations. Another point of interest is that, although olfactory effects (olfactory sickness) were present in early sensory-processing areas, visual effects (visual sickness) seemed to involve higher-order, potentially face-processing, areas, such as the superior and middle frontal gyrus, middle cingulate gyrus, insula, and amygdala. This difference may be interesting to address in further studies in which a higher temporal resolution (i.e., simultaneous EEG and fMRI measurements) would enable targeting of the temporal aspects of sickness signal processing, potentially showing that odor cues serve disease avoidance at very early, and possibly nonconscious stages of perception.

Summarized, the activations in the extended face-processing network and areas responsible for enabling shared experience in an observer may represent a second neural circuitry with clear associations to disease avoidance at the behavioral level. Future studies should use explicit tests of approach–avoidance behavior related to sickness cues (olfactory, visual).

It should be noted that the neural profiles for olfactory sickness and visual sickness showed an expected overlap with the activation pattern relating to the contrast testing for olfactory–visual sickness (e.g., the middle and superior frontal gyrus, OFC, and MDT) (Fig. 4*A*). That exposure to multisensory sickness signals caused an activation of both cortical and subcortical areas supports the idea that sickness detection is related to the detection of one or several sickness signals (the addition model) rather than to the detection of a reduction of one or several health signals (the reduction model) (34). This addition model is supported further by the fact that the reverse contrast (testing olfactory–visual health) revealed no significant activation, even when tested against a very liberal statistical threshold ($P < 0.001$, uncorrected). Although these models are conceptually hard to discriminate, the data presented here are in line with disease detection being more related to the detection of cues signaling sickness than to the detection of a reduced health signal.

Apart from overlapping neural profiles for olfactory, visual, and olfactory–visual sickness cues, olfactory–visual sickness exclusively activated the temporal pole, stretching to the inferior frontal gyrus, and the cerebellum. Although these activations could be related to multisensory enhancement of sickness cues (35), a clear interpretation is hindered by the fact that the contrast olfactory–visual sickness also allows for additive effects of unisensory olfactory and visual sickness cues (36). To focus on the neural signature of clear multisensory enhancement as a correlate of superadditive and modality-independent threat perception, we carried out a contrast that statistically tested the criterion of superadditivity. Superadditive sickness (Fig. 4*B*) yielded activation in the lingual and middle occipital gyrus, in a widespread cluster within the parietal cortex (superior and inferior parietal gyrus and the IPS) and in the motor cortex and the cerebellum. Several areas of this network may represent multisensory integration hubs at both earlier (lingual and middle occipital gyrus) (37) and later (IPS) stages (38, 39) in the perception stream. Given that these activations are reported mainly in studies targeting audiovisual integration (but see ref. 40), we argue that the present findings add olfactory–visual integration

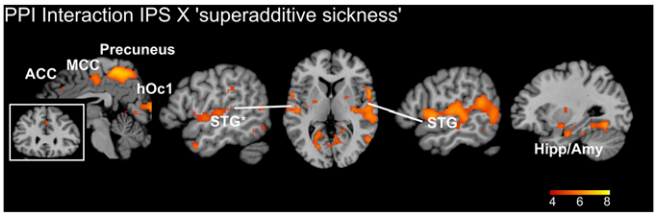

Fig. 5. Whole-brain functional connectivity of IPS and superadditive sickness (*t* test from a random-effects GLM, $T > 4.83$, FWE peak-level corrected, $P < 0.05$). Color bars depict t-values of local maxima peak activation. The asterisk indicates that activation of this cluster also encompassed the inferior temporal gyrus and fusiform gyrus. ACC, anterior cingulate cortex; Hipp/Amy, hippocampus/amygdala; hOc1, primary visual cortex; IPL, inferior parietal lobe; MCC, middle cingulate cortex; STG, superior temporal gyrus.

of human sickness cues into these multisensory convergence zones and represent an activation network that is distinct from its unisensory contributions, olfactory sickness and visual sickness.

The concept of multisensory integration should be interpreted with care, given the limit of the fMRI technique that measures population-based activity rather than single-neuron activity in which the concept was first demonstrated (36, 41). However, the study's validity is supported by the use of the most conservative contrast discussed in the literature [superadditivity (36)]. Moreover, ratings indicated how perceptually subtle, or weak, the sickness cues were, thus suggesting that inverse effectiveness [a greater benefit of multisensory integration for weak unisensory cues (42)] is likely to apply (43).

Importantly, the superior temporal sulcus (STS), and superior temporal gyrus (STG) are considered core areas for multisensory integration (17, 38), including for olfactory–visual integration (44). The STS was significantly connected to the IPS during multisensory integration, as indicated by the PPI analysis (Fig. 3) focusing on functional connectivity of IPS and whole-brain activation. Likewise, the anterior and middle cingulate cortex, precuneus, and hippocampus/amygdala were activated when testing sickness-cue integration-related whole-brain functional connectivity with the IPS but were not activated when previously testing for unisensory odor or face sickness perception. In this context, hippocampus/amygdala activation may represent the involvement of an associative neural network responding to threat (24) represented by a multisensory sickness signal. This notion supports the earlier assumption of olfactory-sickness–driven OFC and MDT activation, suggested to be part of a neural circuitry serving disease avoidance. Last, the middle cingulate cortex has recently been found to exhibit enhanced connectivity with the anterior insula during a first-hand experience of LPS-induced inflammation (26), and this enhancement has been interpreted as a potential neurophysiological mechanism involved in the brain's sickness response. Applied to the current data, the middle cingulate cortex, in the context of multisensory-sickness–driven associations between IPS and whole-brain activations, may indicate a shared representation of an inflammatory state and associated discomfort.

In conclusion, the present study shows how subtle and early olfactory and visual sickness cues interact through cortical activation and may influence humans' approach–avoidance tendencies. The study provides support for sensory integration of information from cues of visual and olfactory sickness in cortical multisensory convergences zones as being essential for the detection and evaluation of sick individuals. Both olfaction and vision, separately and following sensory integration, may thus be important parts of circuits handling imminent threats of contagion, motivating the avoidance of sick conspecifics (3, 5).

Materials and Methods

Participants. Thirty right-handed healthy participants (15 females, 18–34 y of age) participated in the fMRI study. Participants provided written informed consent and were remunerated with movie vouchers. The study conformed to the Declaration of Helsinki and was approved by the regional ethics review board in Stockholm, Sweden. For further details, please see *SI Materials and Methods*.

Stimuli and Stimulus Delivery. Stimuli consisted of combined olfactory–visual presentations. Stimuli had been acquired in a separate study (22) (see also *SI Materials and Methods*). Briefly, 22 healthy males and female individuals, referred to as "donors," had participated in a within-subject double-blind placebo-controlled crossover design that had assessed multiple outcome parameters of one-dose LPS treatment (2.0 ng/kg body weight) or one-dose saline (placebo) control treatment. Please refer to Fig. S2 to see the effects of LPS administration on measures of sickness in comparison to saline administration on the donor sample.

Visual stimuli were static images of 18 selected donor's faces showing neutral facial expression (see *SI Materials and Methods* for further details) taken 2 h after LPS treatment (sick) or placebo treatment (healthy), respectively. The images were visible to participants via an angled mirror mounted on the head coil. Olfactory stimuli were body odor samples of the donors obtained via nursing pads sewn into the left and right armpit area of t-shirts (45) that had been worn for 5 h following LPS (sick) or saline (healthy) injection. An unused sampling pad served as control odor. Olfactory stimuli were presented orthonasally by a computer-controlled 16-channel MR-compatible olfactometer (46). Also see *SI Materials and Methods*.

Experimental Task. The protocol consisted of visual and olfactory stimulus presentations in a 2 × 3 (faces × odors) factorial design during two fMRI sessions (Fig. 6). Participants were asked to focus on the faces rather than on the odors because the latter were often too weak to perceive. They were instructed to rate their liking of the person pictured, inviting them to express their integrated experience. To avoid any perception bias associated with the concept of sickness, participants were not aware that they would be seeing and smelling sick and healthy people. For an example of a photograph of one female donor please refer to Fig. S3.

One trial (Fig. 6) started with the presentation of a black fixation cross (jittered 1,250–2,500 ms duration), which changed color to green (jittered 750–1,000 ms duration) signaling the start of a new breathing cycle ("inhale") to the participant. As the participants inhaled, a face and an odor were presented for 2,000 ms, followed by a 1,000-ms blank screen. A seven-point rating scale ("How much do you like this person?") was then presented for 4,500 ms. The screen cursor could be moved to the right (toward 6, very much) and left (toward 0, not at all) using the ring and index fingers, respectively, and the answer was confirmed with the middle finger, using a MRI-compatible button box.

The same odor (sick or healthy body odor from a male or female donor) or control air was used in three consecutive trials aiming to intensify the otherwise very weak olfactory experience while three different faces were presented. These three faces depicted either a sick or a healthy person (matching sex of the respective body odor). For a detailed description of presentation scheme please refer to *SI Materials and Methods*. Each face image was presented for 2,000 ms, and participants were asked to rate how much they liked the person (from 0, not at all to 6, very much).

After the scanning, participants performed perceptual ratings in the scanner for separately presented face and odor stimuli. All 36 faces (18 sick, 18 healthy) were presented for 2 s each, with a 10-s intertrial rest period; no odor was presented. Participants rated the faces regarding attractiveness on a scale from −3 (very unattractive) to +3 (very attractive), health from −3 (very sick) to +3 (very healthy), and desired social interaction from −3 (not at all desired) to +3 (very much desired). All nine odor pads were presented for 2 s each, with a 30-s intertrial rest period. Participants rated the odors regarding intensity from 0 (not intense at all) to 6 (very intense), pleasantness from −3 (very unpleasant) to +3 (very pleasant), and health from −3 (very sick) to +3 (very healthy). The order of stimuli and rating prompts was randomized.

Data Acquisition and Analysis. Functional images were acquired with a T2*-weighted, gradient-echo, echoplanar imaging (EPI) sequence with a BOLD contrast on a 3T GE (General Electric) 750 MR scanner using an eight-channel head coil.

Data were preprocessed (FieldMap correction, realignment, coregistration and unified segmentation of mean functional image, normalization, and 9-mm smoothing) using SPM8. Data then were analyzed in subjectwise general linear models (GLMs), and contrasts of interest then were analyzed with two mixed-effects GLMs (GLM-1 and GLM-2) for group effects.

In GLM-1, the contrast visual sickness (Fig. 5) compared all presentations of sick faces with all presentations of healthy faces ($V_SO_S+V_SO_H+V_SO_C > V_HO_S+V_HO_H+V_HO_C$), olfactory sickness contrasted all presentations with a sick body odor against all presentations with a healthy body odor ($V_SO_S+V_HO_S > V_SO_H+V_HO_H$), and olfactory–visual sickness contrasted the olfactory–visual sickness condition with that of the multisensory olfactory–visual health condition

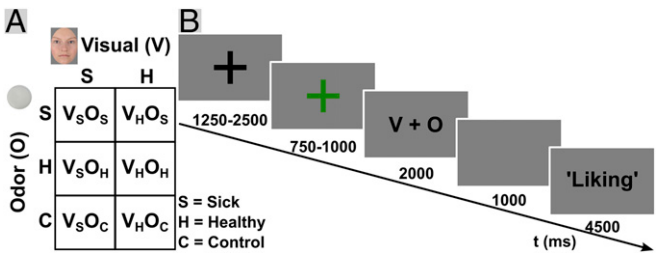

Fig. 6. Description of the study design. (*A*) Face images and odor stimuli were presented simultaneously within a factorial 2 × 3 (faces × odors) design. (*B*) Description of one single trial, including fixation cross, stimulus presentation and a liking rating. C, control odor; H, healthy; S, sick.

($V_SO_S > V_HO_H$). The resulting statistical parametrical maps were thresholded with a combined height and extent threshold technique based on Monte-Carlo simulations (47) and the spatial properties of the residual image [$P < 0.001$, extent threshold of $k = 44$ voxels, corresponding to a cluster-level familiywise error (FWE) of $P < 0.05$]. In GLM-2, the contrast superadditive sickness contrasted the olfactory–visual condition against the sum of the subtraction contrasts. This contrast was thresholded with a peak-level FWE correction of $P < 0.05$ and an extent threshold of $k = 10$ voxels.

For the PPI analysis, we analyzed task-related (superadditive sickness) whole-brain connectivity with an activation hub of interest in the right IPS. The contrast IPS × superadditive sickness was built as in GLM-2 and represented task-related connectivity of the IPS with superadditive sickness. The contrast was also thresholded with a peak-level FWE correction of $P < 0.05$ and an extent threshold of $k = 10$ voxels.

For details of the recording protocol, preprocessing, and analyses, please see *SI Materials and Methods*.

ACKNOWLEDGMENTS. We thank Maria Garke for contributions during data collection and Jonathan Berrebi and Rouslan Sitnikov for optimizing the scan protocol. This research was supported by Deutscher Akademischer Austauschdienst Postdoctoral Fellowship 91518477 (to C.R.), Swedish Research Council Grants 2012-1125 and 2016-02742 (to M.J.O.), Swedish Foundation for Humanities and Social Sciences Grant P12-1017 (to M.J.O.), the Knut and Alice Wallenberg Foundation Grant KAW 2012.0141 (to J.N.L.), and Swedish Research Council Grant 2014-1346 (to J.N.L.).

1. Cohen S, Doyle WJ, Skoner DP, Rabin BS, Gwaltney JM, Jr (1997) Social ties and susceptibility to the common cold. *JAMA* 277:1940–1944.
2. Fumagalli M, et al. (2011) Signatures of environmental genetic adaptation pinpoint pathogens as the main selective pressure through human evolution. *PLoS Genet* 7:e1002355.
3. Schaller M, Park JH (2011) The behavioral immune system (and why it matters). *Curr Dir Psychol Sci* 20:99–103.
4. Shattuck EC, Muehlenbein MP (2015) Human sickness behavior: Ultimate and proximate explanations. *Am J Phys Anthropol* 157:1–18.
5. Stevenson RJ, et al. (2012) Disgust elevates core body temperature and up-regulates certain oral immune markers. *Brain Behav Immun* 26:1160–1168.
6. Arakawa H, Cruz S, Deak T (2011) From models to mechanisms: Odorant communication as a key determinant of social behavior in rodents during illness-associated states. *Neurosci Biobehav Rev* 35:1916–1928.
7. Stephen ID, Coetzee V, Law Smith M, Perrett DI (2009) Skin blood perfusion and oxygenation colour affect perceived human health. *PLoS One* 4:e5083.
8. Schaller M, Miller GE, Gervais WM, Yager S, Chen E (2010) Mere visual perception of other people's disease symptoms facilitates a more aggressive immune response. *Psychol Sci* 21:649–652.
9. Shirasu M, Touhara K (2011) The scent of disease: Volatile organic compounds of the human body related to disease and disorder. *J Biochem* 150:257–266.
10. Moshkin M, et al. (2012) Scent recognition of infected status in humans. *J Sex Med* 9:3211–3218.
11. Dantzer R, O'Connor JC, Freund GG, Johnson RW, Kelley KW (2008) From inflammation to sickness and depression: When the immune system subjugates the brain. *Nat Rev Neurosci* 9:46–56.
12. Olsson MJ, et al. (2014) The scent of disease: Human body odor contains an early chemosensory cue of sickness. *Psychol Sci* 25:817–823.
13. Sundelin T, et al. (2015) Sick man walking: Perception of health status from body motion. *Brain Behav Immun* 48:53–56.
14. de Groot JH, Smeets MA, Kaldewaij A, Duijndam MJ, Semin GR (2012) Chemosignals communicate human emotions. *Psychol Sci* 23:1417–1424.
15. Lundström JN, Olsson MJ (2005) Subthreshold amounts of social odorant affect mood, but not behavior, in heterosexual women when tested by a male, but not a female, experimenter. *Biol Psychol* 70:197–204.
16. Mujica-Parodi LR, et al. (2009) Chemosensory cues to conspecific emotional stress activate amygdala in humans. *PLoS One* 4:e6415.
17. Stein BE, Stanford TR (2008) Multisensory integration: Current issues from the perspective of the single neuron. *Nat Rev Neurosci* 9:255–266.
18. Stein BE, Stanford TR, Rowland BA (2014) Development of multisensory integration from the perspective of the individual neuron. *Nat Rev Neurosci* 15:520–535.
19. Stevenson RA, et al. (2014) Identifying and quantifying multisensory integration: A tutorial review. *Brain Topogr* 27:707–730.
20. Cialdini R, Trost M (1998) Social influence: Social norms, conformity, and compliance. *The Handbook of Social Psychology*, eds Gilbert D, Fiske S, Lindzey G (McGraw-Hill, Boston), 4th Ed, Vol 2, pp 151–192.
21. Cialdini RB, Goldstein NJ (2004) Social influence: Compliance and conformity. *Annu Rev Psychol* 55:591–621.
22. Lasselin J, et al. (2017) Lipopolysaccharide alters motivated behavior in a monetary reward task: A randomized trial. *Neuropsychopharmacology* 42:801–810.
23. Henderson AJ, et al. (2017) Skin colour changes during experimentally-induced sickness. *Brain Behav Immun* 60:312–318.
24. Li W (2014) Learning to smell danger: Acquired associative representation of threat in the olfactory cortex. *Front Behav Neurosci* 8:98.
25. Vuilleumier P, Driver J (2007) Modulation of visual processing by attention and emotion: Windows on causal interactions between human brain regions. *Philos Trans R Soc Lond B Biol Sci* 362:837–855.
26. Lekander M, et al. (2016) Intrinsic functional connectivity of insular cortex and symptoms of sickness during acute experimental inflammation. *Brain Behav Immun* 56:34–41.
27. Seubert J, Freiherr J, Djordjevic J, Lundström JN (2013) Statistical localization of human olfactory cortex. *Neuroimage* 66:333–342.
28. Li W, et al. (2010) Right orbitofrontal cortex mediates conscious olfactory perception. *Psychol Sci* 21:1454–1463.
29. Sela L, et al. (2009) Spared and impaired olfactory abilities after thalamic lesions. *J Neurosci* 29:12059–12069.
30. Courtiol E, Wilson DA (2015) The olfactory thalamus: Unanswered questions about the role of the mediodorsal thalamic nucleus in olfaction. *Front Neural Circuits* 9:49.
31. Kühn S, Gallinat J (2012) The neural correlates of subjective pleasantness. *Neuroimage* 61:289–294.
32. Ishai A, Schmidt CF, Boesiger P (2005) Face perception is mediated by a distributed cortical network. *Brain Res Bull* 67:87–93.
33. Lamm C, Decety J, Singer T (2011) Meta-analytic evidence for common and distinct neural networks associated with directly experienced pain and empathy for pain. *Neuroimage* 54:2492–2502.
34. Penn D, Potts WK (1998) Chemical signals and parasite-mediated sexual selection. *Trends Ecol Evol* 13:391–396.
35. Olson IR, Plotzker A, Ezzyat Y (2007) The enigmatic temporal pole: A review of findings on social and emotional processing. *Brain* 130:1718–1731.
36. Beauchamp MS (2005) Statistical criteria in FMRI studies of multisensory integration. *Neuroinformatics* 3:93–113.
37. Macaluso E, Frith CD, Driver J (2000) Modulation of human visual cortex by crossmodal spatial attention. *Science* 289:1206–1208.
38. Driver J, Noesselt T (2008) Multisensory interplay reveals crossmodal influences on 'sensory-specific' brain regions, neural responses, and judgments. *Neuron* 57:11–23.
39. Calvert GA, Campbell R, Brammer MJ (2000) Evidence from functional magnetic resonance imaging of crossmodal binding in the human heteromodal cortex. *Curr Biol* 10:649–657.
40. Osterbauer RA, et al. (2005) Color of scents: Chromatic stimuli modulate odor responses in the human brain. *J Neurophysiol* 93:3434–3441.
41. Laurienti PJ, Perrault TJ, Stanford TR, Wallace MT, Stein BE (2005) On the use of superadditivity as a metric for characterizing multisensory integration in functional neuroimaging studies. *Exp Brain Res* 166:289–297.
42. Stein BE, Stanford TR, Ramachandran R, Perrault TJ, Jr, Rowland BA (2009) Challenges in quantifying multisensory integration: Alternative criteria, models, and inverse effectiveness. *Exp Brain Res* 198:113–126.
43. Werner S, Noppeney U (2010) Superadditive responses in superior temporal sulcus predict audiovisual benefits in object categorization. *Cereb Cortex* 20:1829–1842.
44. Novak LR, Gitelman DR, Schuyler B, Li W (2015) Olfactory-visual integration facilitates perception of subthreshold negative emotion. *Neuropsychologia* 77:288–297.
45. Lundström JN, Boyle JA, Zatorre RJ, Jones-Gotman M (2008) Functional neuronal processing of body odors differs from that of similar common odors. *Cereb Cortex* 18:1466–1474.
46. Lundström JN, Gordon AR, Alden EC, Boesveldt S, Albrecht J (2010) Methods for building an inexpensive computer-controlled olfactometer for temporally-precise experiments. *Int J Psychophysiol* 78:179–189.
47. Eklund A, Nichols TE, Knutsson H (2016) Cluster failure: Why fMRI inferences for spatial extent have inflated false-positive rates. *Proc Natl Acad Sci USA* 113:7900–7905.
48. Willenbockel V, et al. (2010) Controlling low-level image properties: The SHINE toolbox. *Behav Res Methods* 42:671–684.
49. Hummel T, Konnerth CG, Rosenheim K, Kobal G (2001) Screening of olfactory function with a four-minute odor identification test: Reliability, normative data, and investigations in patients with olfactory loss. *Ann Otol Rhinol Laryngol* 110:976–981.
50. Hummel T, Kobal G, Gudziol H, Mackay-Sim A (2007) Normative data for the "Sniffin' Sticks" including tests of odor identification, odor discrimination, and olfactory thresholds: An upgrade based on a group of more than 3,000 subjects. *Eur Arch Otorhinolaryngol* 264:237–243.
51. Faul F, Erdfelder E, Lang AG, Buchner A (2007) G*Power 3: A flexible statistical power analysis program for the social, behavioral, and biomedical sciences. *Behav Res Methods* 39:175–191.
52. Cumming G (2012) *Understanding the New Statistics: Effect Sizes, Confidence Intervals, and Meta-Analysis* (Taylor & Francis, Oxford, UK).
53. Hutton C, et al. (2002) Image distortion correction in fMRI: A quantitative evaluation. *Neuroimage* 16:217–240.
54. Andersson JLR, Hutton C, Ashburner J, Turner R, Friston K (2001) Modeling geometric deformations in EPI time series. *Neuroimage* 13:903–919.
55. Ashburner J, Friston KJ (2005) Unified segmentation. *Neuroimage* 26:839–851.
56. Eickhoff SB, et al. (2005) A new SPM toolbox for combining probabilistic cytoarchitectonic maps and functional imaging data. *Neuroimage* 25:1325–1335.
57. Hayes DJ, Huxtable AG (2012) Interpreting deactivations in neuroimaging. *Front Psychol* 3:27.
58. Rolls ET, Grabenhorst F, Parris BA (2010) Neural systems underlying decisions about affective odors. *J Cogn Neurosci* 22:1069–1082.
59. Andreasson A, et al. (July 24, 2016) A global measure of sickness behaviour: Development of the Sickness Questionnaire. *J Health Psychol*, 10.1177/1359105316659917.
60. Eickhoff SB, et al. (2007) Assignment of functional activations to probabilistic cytoarchitectonic areas revisited. *Neuroimage* 36:511–521.